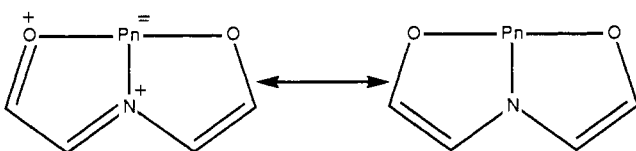


fluorides also show the opposite periodic trend in the inversion barriers with SbF_3 having the lowest edge inversion barrier. Thus the barriers decrease with increasing pnictogen atomic number, and, in fact, the difference is approximately constant in contrast to the leveling effect observed for the hydrides. The ΔZPE correction to the edge inversion barriers for the fluorides is again small being -0.9 kcal/mol for PF_3 , -0.6 kcal/mol for AsF_3 , and -0.4 kcal/mol for SbF_3 . The final corrected, correlated barriers for edge inversion in the fluorides are 52.9, 45.7, and 38.3 kcal/mol for PF_3 , AsF_3 , and SbF_3 , respectively. It is of interest to note that the edge inversion barrier for SbF_3 is actually lower than the vertex inversion barrier for SbH_3 .

The decrease in the edge inversion barrier with increasing pnictogen atomic number is not surprising and correlates well with the increasing stability for increasing pnictogen atomic number observed for ADPnO complexes which have a T-shaped structure.²⁸



(28) (a) Culley, S. A.; Arduengo, A. J., III. *J. Am. Chem. Soc.* **1984**, *106*, 1164. (b) Culley, S. A.; Arduengo, A. J., III. *J. Am. Chem. Soc.* **1985**, *107*, 1089. (c) Stewart, C. A.; Harlow, R. L.; Arduengo, A. J., III. *J. Am. Chem. Soc.* **1985**, *107*, 5543. (d) Arduengo, A. J., III.; Stewart, C. A.; Davidson, F.; Dixon, D. A.; Becker, J. Y.; Culley, S. A.; Mizen, M. B. *J. Am. Chem. Soc.*, in press.

Our SCF inversion barrier for PF_3 for vertex inversion through the D_{3h} transition state is in reasonable agreement with the value found by Marynick^{25a} of 121.5 kcal/mol considering the differences in geometries and basis sets. For AsF_3 , our SCF calculation is with a much larger basis set and with much better geometries. Marynick's value²⁷ of 111.9 kcal/mol is 15.6 kcal/mol higher in energy than our value showing the necessity of a good basis set and a good set of geometries in these calculations.

Finally, returning to the observation that the T-shaped C_{2v} structures for the hydrides are minima on a potential energy hypersurface,²⁹ we note that these structures may be accessed by electronic excitation. Including corrections for ΔZPE , the 0-0 transition of these states are calculated to be at 158.1 (55, 335 cm^{-1}), 140.6 (49, 210 cm^{-1}), and 112.4 (39, 340 cm^{-1}) kcal/mol above the ground state. The observed absorption spectra³⁰ are quite complex and have been assigned to Rydberg transitions. We do note that the continuous absorption in PH_3 has the maximum intensity at 1800 Å (55, 556 cm^{-1}) which is in an energy region consistent with our result. However, for AsH_3 , the maximum is at 1830 Å (54, 645 cm^{-1}) which is higher than our result. For SbH_3 , the continuum has a maximum intensity at 1970 Å (50, 781 cm^{-1}), clearly much higher than our value. However, it would seem useful to reinvestigate the UV spectra of these hydrides to look for evidence of the states having C_{2v} structure.

(29) The T-shaped C_{2v} structures for the hydrides were calculated with an in-plane lone pair. If the lone pair is an out-of-plane p orbital then the C_{2v} structure is simply a distorted D_{3h} structure.

(30) Humphries, C. M.; Walsh, A. D.; Warsop, P. A. *Disc. Faraday Soc.* **1963**, *35*, 137.

Steric Effects on Atropisomerism in Tetraarylporphyrins

Maxwell J. Crossley, Leslie D. Field, Adrienne J. Forster, Margaret M. Harding, and Sever Sternhell*

Contribution from the Department of Organic Chemistry, The University of Sydney, N.S.W. 2006, Australia. Received March 13, 1986

Abstract: The rate of aryl ring rotation in a series of 5,10,15,20-tetrakis(2-X-5-methoxyphenyl)porphyrins, where X = H, F, Cl, Br, and I, was studied by NMR spectroscopy and chromatography. Where X = Cl, Br, and I, the four atropisomers $\alpha\beta\alpha\beta$, $\alpha\alpha\beta\beta$, $\alpha\alpha\alpha\beta$, and $\alpha\alpha\alpha\alpha$ were isolated and were stable at 298 K. When X = H or F, facile interconversion of the atropisomers at 298 K prevented isolation of pure atropisomers, but for X = F samples of >80% isomeric purity were isolated at low temperatures. The approach of nonequilibrated mixtures of atropisomers to equilibrium at elevated temperatures was monitored by HPLC experiments for X = Cl, Br, and I, and ^{19}F NMR spectroscopy for X = F. Rate constants were obtained for the six processes by which the atropisomers can interconvert. The rotational barriers increased monotonically as the van der Waals radii of the substituent X. The rotational barriers were correlated with the "apparent overlap" of the ortho substituents, Σr^* , a geometric parameter previously proposed to quantify steric interactions on the internal rotation in biaryls.

Biphenyl-type atropisomerization in ortho-substituted tetraarylporphyrins was first reported by Gottwald and Ullmann¹ who separated the atropisomers of 5,10,15,20-tetrakis(o-hydroxyphenyl)porphyrin. X-ray structures of several 5,10,15,20-tetraarylporphyrins show that the aryl rings are inclined roughly perpendicular (60–90°) to the plane of the porphyrin ring in both free-base and metallo derivatives in the solid state,² and thus the ortho substituents project above and below the porphyrin plane. Aryl ring rotation in solution has been shown to be slow

on the NMR time scale at ambient temperature, and the aryl ring, on average, is orthogonal to the plane of the porphyrin.³ The atropisomerism, due to restricted rotation of the aryl rings about the porphyrin-arene bond, gives rise to four atropisomers (e.g., Figure 1). In an equilibrated mixture the four atropisomers $\alpha\beta\alpha\beta$, $\alpha\alpha\beta\beta$, $\alpha\alpha\alpha\beta$, and $\alpha\alpha\alpha\alpha$ are present in the statistical ratio of 1:2:4:1, respectively.

The restricted rotation which results when an amido substituent is placed on the ortho positions of the meso aryl rings has been exploited in the design and synthesis of a number of chemical models for heme-containing biological systems.⁴ On the basis

(1) Gottwald, L. K.; Ullman, E. F. *Tetrahedron Lett.* **1969**, 3071.

(2) Fleischer, E. B. *Acc. Chem. Res.* **1970**, *3*, 105. Hoard, J. L. *Porphyrins and Metalloporphyrins*; Smith, K. M., Ed.; Elsevier: Amsterdam, 1975; p 317.

(3) Scheer, H., and Katz, J. K. In ref 2, p 399.

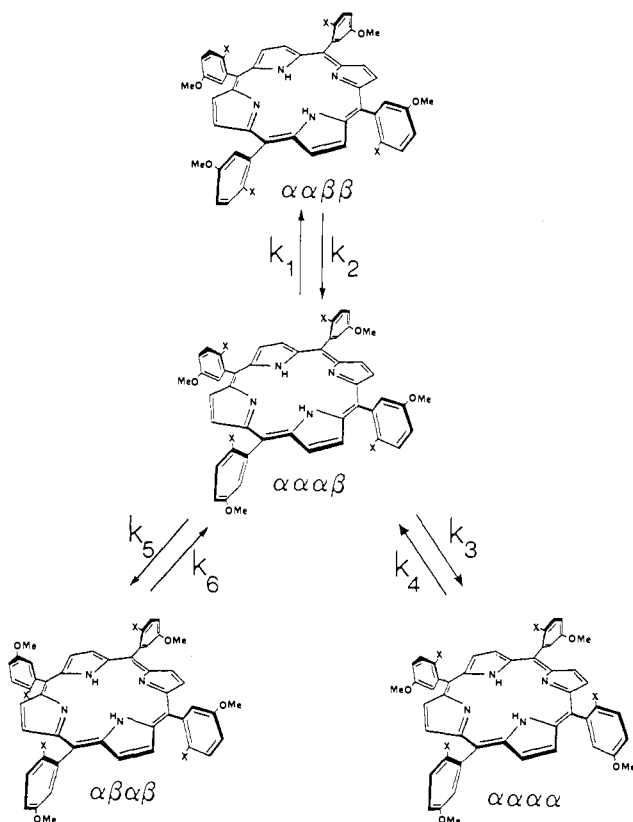


Figure 1. Atropisomerism in 5,10,15,20-tetrakis(2-X-5-methoxyphenyl)porphyrins.

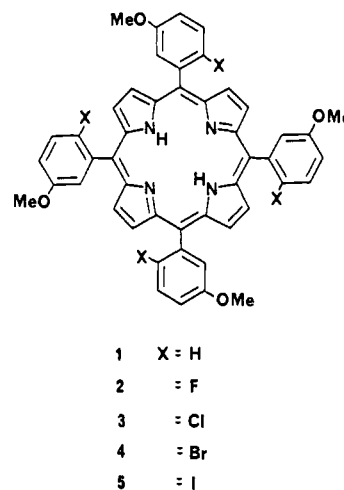
of these studies it seems that porphyrin systems with other ortho substituents on the meso aryl rings could prove to be very useful precursors for related chemical models for hemoproteins. Thus, the importance to planning and synthesis of being able to accurately predict the stability of atropisomers is self-evident.

We have previously shown that in 2,2'-disubstituted biphenyls and related systems, the rate of rotation of one aryl ring with respect to another is quantitatively related to the "steric size" of the ortho substituents.⁵ Internal rotation in biaryls involves a transition state where the aryl rings are coplanar, and substantial deformation of bond angles and bond lengths must occur in the transition state to allow the ortho substituents to pass one another. A simple geometric parameter, Σr^* (the "apparent overlap" of the ortho substituents), which is related to the deformation which a molecule must undergo in order to accomplish the conformational change, was found to have a good linear correlation with the experimentally determined barriers.⁵

As in the case of biaryls,⁵ the rate of interconversion of porphyrin atropisomers should be a function of the steric size of the ortho substituent on the aryl rings. This appears to be so, qualitatively at least, from the available data on free-base 5,10,15,20-tetrakis(ortho-substituted-phenyl)porphyrins in which the rotational barriers decrease as the size of the ortho substituent in the order $\text{NHCOCMe}_3^6 < \text{NHCO}(\text{CH}_2)_{15}\text{Me}^6 = \text{NHCOEt}^6 < \text{CN}^7 < \text{OMe}^8 < \text{OH}^1$. Data on porphyrin dications^{6,8} and

metalloporphyrins^{6,9} are also in agreement with this trend, although a direct comparison of these rotational barriers with barriers in free-base porphyrins should not be made since the ground-state and transition-state interactions differ considerably.^{2,6,8,9}

In order to quantify steric effects on atropisomerism in porphyrin systems, we have studied aryl ring rotation in a series of 5,10,15,20-tetrakis(2-X-5-methoxyphenyl)porphyrins where X = H, F, Cl, Br, and I (1–5). A methoxy group was incorporated



in the 5-position of the aryl rings to simplify the aromatic region of the NMR spectrum and as a suitable group to monitor the atropisomer by NMR spectroscopy. Projected calculations, based on the parameter Σr^* , indicated that the rotational barriers for 1–5 would range from approximately 80 to 140 $\text{kJ}\cdot\text{mol}^{-1}$ and increase monotonically as the substituent X was varied from hydrogen to iodine. For the bulkier substituents, the rotational barriers were predicted to be $> 120 \text{ kJ}\cdot\text{mol}^{-1}$, i.e., outside the range accessible to dynamic NMR spectroscopy. The tetraarylporphyrin system was thus an excellent model to test the generality of the apparent overlap theory in a framework different from that of the biphenyls and also provided information on the stability and dynamics of the atropisomers of ortho-substituted tetraarylporphyrins.

Results

Synthesis of Porphyrins and Separation of Atropisomers. All porphyrins in the series were prepared by the Rothmund condensation of pyrrole with the appropriate 2-X-5-methoxybenzaldehyde in boiling propionic acid. Porphyrins 2, 4, and 5 crystallized directly from the appropriate reaction mixture, in yields ranging from 3 to 12%, decreasing with the size of the ortho substituents. For X = Cl (3), pure $\alpha\alpha\beta\beta$ atropisomer crystallized preferentially from the reaction mixture in 1% yield. Further porphyrin was obtained as a mixture of the four atropisomers by concentration and extraction of the mother liquor, to give a total yield of 7%.

Four distinct bands were observed by TLC for porphyrins 3, 4, and 5, and chromatography on silica allowed isolation of the four atropisomers. In order of elution they were obtained in the approximate ratio of 1:2:4:1 and were assigned in order of increasing polarity as $\alpha\beta\alpha\beta < \alpha\alpha\beta\beta < \alpha\alpha\alpha\beta < \alpha\alpha\alpha\alpha$. These assignments were confirmed by NMR spectroscopy (see below). When X = F (2), distinct bands corresponding to the four atropisomers were not observed by TLC at room temperature. Chromatography at temperature less than 10 °C allowed the isolation of samples enhanced in each isomer. Pure atropisomers could not be isolated, but samples of ca. 80% isomeric purity could be obtained and stored successfully in liquid nitrogen for several days without reequilibration.

(4) (a) Collman, J. P.; Gagne, R. R.; Reed, C. A.; Halbert, T. R.; Lang, G.; Robinson, W. T. *J. Am. Chem. Soc.* **1975**, *97*, 1427. (b) Collman, J. P.; Brauman, J. I.; Doxsee, K. M.; Halbert, T. R.; Bunnenberg, E.; Linder, R. E.; LaMar, G. N.; Del Gaudio, J.; Lang, G.; Spartalian, K. *Ibid.* **1980**, *102*, 4182. (c) Collman, J. P.; Groh, S. E. *Ibid.* **1982**, *104*, 1391. (d) Groves, J. T.; Myers, R. S. *Ibid.* **1983**, *105*, 5791. (e) Mansuy, M.; Battione, P.; Renaud, J.-P.; Guerin, P., *J. Chem. Soc., Chem. Commun.* **1985**, 155. (f) Boitrel, B.; Lecas, A.; Renko, Z.; Rose, E. *Ibid.* **1985**, 1820. (g) Walker, F. A.; Buehler, J.; West, J. T.; Hinds, J. L. *J. Am. Chem. Soc.* **1983**, *105*, 6923.

(5) Bott, G.; Field, L. D.; Sternhell, S. *J. Am. Chem. Soc.* **1980**, *102*, 5618. (6) Freitag, R. A.; Mercer-Smith, J. A.; Whitten, D. G. *J. Am. Chem. Soc.* **1981**, *103*, 1226. Freitag, R. A.; Whitten, D. G. *J. Phys. Chem.* **1983**, *87*, 3918.

(7) Hatano, K.; Anzai, K.; Kubo, T.; Tamai, S. *Bull. Chem. Soc. Jpn.* **1981**, *54*, 3518.

(8) Dirks, J. W.; Underwood, G.; Matheson, J. C.; Gust, D. *J. Org. Chem.* **1979**, *44*, 2551.

(9) Walker, F. A.; Avery, G. L. *Tetrahedron Lett.* **1971**, 4949.

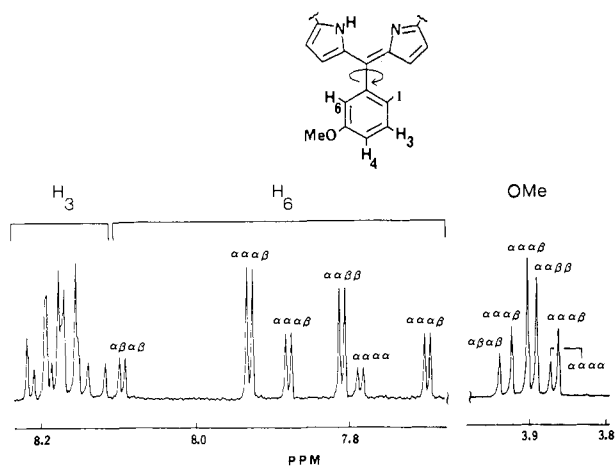


Figure 2. Portion of the 400-MHz ^1H NMR spectrum of a mixture of the four atropisomers of 5,10,15,20-tetrakis(2-iodo-5-methoxyphenyl)porphyrin (**5**): dimethyl- d_6 sulfoxide, 298 K. $\alpha\beta\alpha\beta/\alpha\alpha\beta\beta/\alpha\alpha\alpha\beta/\alpha\alpha\alpha\alpha = 9:25:59:7$.

Synthesis of the iodo- and fluoroporphyrins **5** and **2** required the development of syntheses of the precursor benzaldehydes. 2-Iodo-5-methoxybenzaldehyde (**6**) was prepared by iodination of *m*-methoxybenzaldehyde with iodine and silver trifluoroacetate. Attempted iodination of *m*-hydroxybenzaldehyde prior to methylation according to the literature method¹⁰ afforded 4-iodo-5-methoxybenzaldehyde in >95% yield, and not the reported 2-iodo-5-methoxybenzaldehyde. The position of iodination was established conclusively by NMR spectroscopy using NOE experiments. An NOE from the methoxyl resonance enhanced H-6 in the 4-substituted aldehyde while NOE was transmitted to H-6 as well as H-4 in the 2-substituted aldehyde.

2-Fluoro-5-methoxybenzaldehyde (**7**) was prepared in three steps from 2-amino-5-methoxytoluene. The amine was converted to its diazonium hexafluorophosphonium salt under Balz-Schiemann conditions,^{11a} and thermal decomposition of the salt afforded 2-fluoro-5-methoxytoluene (**8**) in good yield. Bromination of **8** with *N*-bromosuccinimide and a catalytic amount of benzoyl peroxide in carbon tetrachloride afforded 2-fluoro-5-methoxybenzyl bromide (**9**) which was oxidized to the required aldehyde **7**. Diazotization of 2-amino-5-methoxytoluene with hydrofluoric rather than hydrochloric acid, an alternative procedure to the Balz-Schiemann reaction,^{11a} produced 2-methyl-1,4-benzoquinone as the major product on heating, and no fluorinated product. Presumably hydrofluoric acid was not strong enough to effect amine protonation, and competitive autooxidation to the quinone occurred.^{11b} Attempts to produce the fluoroaldehyde in an analogous manner to the synthesis of the chloro and bromo aldehydes (i.e., starting from 2-fluoro-5-nitrobenzaldehyde) were unsuccessful, as diazotization to produce the precursor phenol led to loss of fluorine from the aromatic ring.

Structural Assignment of Atropisomers. The room-temperature ^1H NMR spectra of porphyrins **2-5** exhibited multiple signals in the methoxyl and aromatic regions of the spectrum which was attributed to porphyrin atropisomerism.

At equilibrium a porphyrin of type **1-5** is expected to exist as a mixture of four diastereomeric conformers, $\alpha\beta\alpha\beta$, $\alpha\alpha\beta\beta$, $\alpha\alpha\alpha\beta$, and $\alpha\alpha\alpha\alpha$, in the statistical ratio of 1:2:4:1 (Figure 1). In the NMR spectrum, when aryl ring rotation is slow on the NMR time scale, each atropisomer gives rise to distinct resonances for each of H-3, H-4, H-6, and -OMe. By its symmetry, the ^1H NMR spectrum of the $\alpha\alpha\alpha\beta$ atropisomer has three types of -OMe and three sets of aromatic protons in the ratio of 1:2:1. All other atropisomers contain only one type of -OMe and one set of aromatic protons. Hence, in an equilibrated mixture of isomers there are six -OMe signals and six resonances for H-3, H-4, and

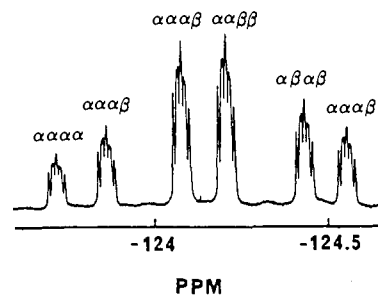


Figure 3. 376.5-MHz ^{19}F NMR spectrum of an equilibrium mixture of the four atropisomers of 5,10,15,20-tetrakis(2-fluoro-5-methoxyphenyl)porphyrin (**2**): CDCl_3 , 298 K.

H-6 in the ratio of 1:2:1:2:1:1. The NMR spectra of porphyrins **2-5**, where X = F, Cl, Br and I, exhibited multiple resonances in each region of the spectrum in approximately the expected ratios (e.g., Figure 2). In all sets of atropisomers the signals for the β -pyrrolic protons were accidentally equivalent.

The assignments of the isomers on polarity considerations were confirmed by the NMR spectra of the individual isomers. The $\alpha\alpha\alpha\beta$ isomer was immediately identified as it gave signals in the ratio 1:2:1 in each region of its ^1H NMR spectrum. The other three isomers showed only one set of signals in each region of the ^1H NMR spectrum although the $\alpha\alpha\beta\beta$ should, in principle, show two sets of β -pyrrolic signals. The $\alpha\alpha\beta\beta$ isomer was distinguished from the $\alpha\alpha\alpha\alpha$ and $\alpha\beta\alpha\beta$ isomers, however, by comparison with a statistically equilibrated mixture of the four isomers where the $\alpha\alpha\beta\beta$ occurs at twice the concentration of both the $\alpha\beta\alpha\beta$ and the $\alpha\alpha\alpha\alpha$ isomers. The $\alpha\beta\alpha\beta$ and $\alpha\alpha\alpha\alpha$ isomers were not able to be assigned on the basis of their NMR spectra and were distinguished on the basis of polarity ($\alpha\alpha\alpha\alpha > \alpha\beta\alpha\beta$). This assignment follows the work of Collman et al., who reported the X-ray crystal structure of an oxygenated iron derivative of the most polar $\alpha\alpha\alpha\alpha$ isomer of 5,10,15,20-tetrakis(*o*-pivalamidophenyl)porphyrin.^{4a}

When X = F (**2**), the ^1H NMR spectrum contained exchange-broadened resonances in the statistical ratio of 1:2:1:2:1:1 in each region of the spectrum which indicated that aryl ring rotation was occurring on the NMR time scale at room temperature. On the basis of polarity and on comparison of the NMR spectra of mixtures enhanced in each atropisomer with the equilibrated mixture of the four atropisomers, the six methoxyl resonances in the NMR spectrum were assigned to the four atropisomers. Similarly, the six proton-coupled resonances in the ^{19}F NMR spectrum were assigned to the four atropisomers (Figure 3).

Measurement of Activation Parameters. The four atropisomers are in equilibrium and can be interconverted by the processes shown in Figure 1.¹² At equilibrium the atropisomers exist in a ratio which reflects their statistical probabilities modified by their relative stabilities. The rate at which nonequilibrium mixtures approach their equilibrium values is defined by six rate constants (k_1 - k_6) which may be expressed by the following equations:

$$-d[\text{A}]/dt = 4k_2[\text{A}] - 2k_1[\text{B}] \quad (1)$$

$$-d[\text{B}]/dt = [\text{B}](2k_1 + k_3 + k_5) - 4(k_2[\text{A}] + k_4[\text{C}] + k_6[\text{D}]) \quad (2)$$

$$-d[\text{C}]/dt = 4k_4[\text{C}] - k_3[\text{B}] \quad (3)$$

$$-d[\text{D}]/dt = 4k_6[\text{D}] - k_5[\text{B}] \quad (4)$$

where A = $\alpha\alpha\beta\beta$, B = $\alpha\alpha\alpha\beta$, C = $\alpha\alpha\alpha\alpha$, and D = $\alpha\beta\alpha\beta$.

For porphyrins **3**, **4**, and **5**, nonequilibrated samples, prepared by chromatography, were heated in hydrocarbon solvents (toluene, xylene, or mesitylene), and their approach to equilibrium was followed with time. Experiments were carried out at three tem-

(10) Hodgson, H.; Smith, E. W. *J. Chem. Soc.* **1937**, 76.

(11) (a) Suschitzky, H. *Adv. Fluorine Chem.* **1965** *4*, 1. (b) Cason, J. *Org. React.* **1948**, *4*, 305.

(12) Processes which involve simultaneous rotation of two or more rings are ignored as they are of low statistical probability, since Whitten and his co-workers⁶ have shown that the thermal isomerization involves a step-by-step one-bond mechanism.

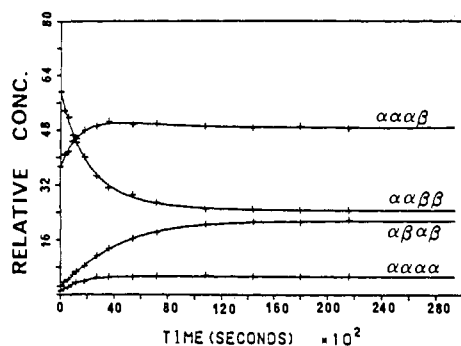


Figure 4. Computer-generated curves of best fit (to eq 1-4) for the recovery to equilibrium of 5,10,15,20-tetrakis(2-chloro-5-methoxyphenyl)porphyrin (3): initial isomer content $\alpha\beta\alpha\beta/\alpha\alpha\beta\beta/\alpha\alpha\alpha\beta/\alpha\alpha\alpha\alpha = 2.5:59.2:37.3:1.0$, toluene, 383 K.

peratures using a sample enhanced in a different atropisomer in each case. Aliquots were removed from the reaction mixture periodically, and the ratio of the atropisomers in a particular sample was determined by analytical HPLC (UV detector). The atropisomers were found to have identical absorption maxima and extinction coefficients (within experimental limits) and hence the percent composition of the sample could be determined directly from the HPLC trace by integration of the areas under each peak. Irrespective of the initial atropisomer composition used in the kinetic experiments, the same equilibrium concentrations resulted. The data from a typical run are shown in Figure 4, the solid lines being the computed curves of best fit to the data described below. In toluene, xylene, and mesitylene, the mixture did not attain the statistical populations of the atropisomers at equilibrium, and the isomeric ratio was approximately $\alpha\beta\alpha\beta:\alpha\alpha\beta\beta:\alpha\alpha\alpha\beta:\alpha\alpha\alpha\alpha = 20:26:48:6$. The NMR spectra of porphyrins heated in dimethyl- d_6 sulfoxide indicated that in the more polar solvent the equilibrium concentration of the atropisomers approximated the statistical ratio. This solvent or other solvents of similar polarity were not used for the kinetic experiments because of their unsuitability for chromatography.

When $X = F$ (2), aryl ring rotation was too rapid at room temperature to permit the equilibration of the atropisomers to be followed by HPLC. The dynamic process was monitored by ^{19}F NMR spectroscopy. This was particularly useful since six base-line-resolved proton-coupled resonances were observed in the ^{19}F spectrum at 376.5 MHz (Figure 3). ^{19}F spectra of disequilibriumed samples were recorded at regular time intervals. The ratio of the atropisomers at a given time was obtained from signal intensities of the peaks where the $\alpha\alpha\alpha\beta$ isomer had contributions from three signals in the ratio 1:2:1.

When $X = H$ (1), the methoxy group gave rise to a sharp singlet in the NMR spectrum in a variety of solvents which suggested, not unexpectedly, rapid interconversion of the atropisomers. The compound was cooled in various solvents in order to slow the isomerization process, and in toluene- d_8 the methoxyl resonance appeared as a broad triplet at 180 K. We attribute this to slow aryl ring rotation at this temperature with the very small difference in magnetic environment of the methoxy group in the four atropisomers resulting in coincident signals. While full kinetic analysis of porphyrin 1 was not possible, an estimate of ΔG^\ddagger at the coalescence temperature (210 ± 20 K) was obtained from the slow-exchange chemical shift difference (10 ± 10 Hz). The relatively large errors associated with these measurements translate to a comparatively small percentage error in the calculation of $\Delta G^\ddagger_{210} = 45 \pm 5$ kJ·mol $^{-1}$, but because of the uncertainty in the estimation of both k and T this value is not included in Table III.

Discussion

The results of the equilibration experiments were fitted by a nonlinear least-squares computer program to the integrated form of eq 1-4 to give the six rate constants which define the isomerization (e.g., Figure 4). The fact that in hydrocarbon solvents nonstatistical ratios of the four atropisomers were obtained indicated that k_1-k_6 were not identical and barriers corresponding

Table I. ΔG^\ddagger Values for Aryl Ring Rotation in Ortho-Substituted Tetraarylporphyrins

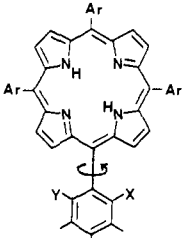
(i) <i>meso</i> -Tetrakis(2-fluoro-5-methoxyphenyl)porphyrin (2)			
ΔG^\ddagger , kJ·mol $^{-1}$	temperature		
	285 K ^b	293 K ^b	298 K ^b
ΔG^\ddagger_1	92.5 \pm 0.7	93.1 \pm 0.8	93.1 \pm 1.3
ΔG^\ddagger_2	92.6 \pm 0.7	93.5 \pm 0.7	93.2 \pm 1.3
ΔG^\ddagger_3	93.0 \pm 0.8	93.7 \pm 0.9	93.8 \pm 0.9
ΔG^\ddagger_4	92.2 \pm 0.8	92.3 \pm 1.0	92.9 \pm 1.0
ΔG^\ddagger_5	92.3 \pm 0.7	92.0 \pm 1.7	92.8 \pm 0.7
ΔG^\ddagger_6	93.0 \pm 0.7	91.9 \pm 1.8	93.5 \pm 0.7
ΔG^\ddagger_7	92.6 \pm 1.2 ^a	93.1 \pm 2.1 ^a	93.2 \pm 1.3 ^a
(ii) <i>meso</i> -Tetrakis(2-chloro-5-methoxyphenyl)porphyrin (3)			
ΔG^\ddagger , kJ·mol $^{-1}$	temperature		
	373 K ^c	383 K ^c	393 K ^d
ΔG^\ddagger_1	126.7 \pm 0.9	124.4 \pm 0.7	127.0 \pm 0.8
ΔG^\ddagger_2	126.4 \pm 0.9	124.7 \pm 0.7	127.0 \pm 0.7
ΔG^\ddagger_3	129.0 \pm 0.9	126.2 \pm 0.9	127.4 \pm 0.9
ΔG^\ddagger_4	126.6 \pm 1.2	124.4 \pm 1.0	124.6 \pm 1.0
ΔG^\ddagger_5	126.8 \pm 0.8	124.1 \pm 0.8	126.9 \pm 0.7
ΔG^\ddagger_6	129.4 \pm 1.1	126.6 \pm 0.9	128.8 \pm 0.8
ΔG^\ddagger_7	127.3 \pm 2.6 ^a	125.3 \pm 2.1 ^a	127.2 \pm 3.0 ^a
(iii) <i>meso</i> -Tetrakis(2-bromo-5-methoxyphenyl)porphyrin (4)			
ΔG^\ddagger , kJ·mol $^{-1}$	temperature		
	383 K ^c	403 K ^d	411 K ^d
ΔG^\ddagger_1	139.0 \pm 18.2 ^f	134.1 \pm 0.8	130.0 \pm 1.3
ΔG^\ddagger_2	136.7 \pm 8.0 ^f	134.3 \pm 0.8	130.9 \pm 1.4
ΔG^\ddagger_3	131.6 \pm 1.3	133.9 \pm 0.8	133.3 \pm 1.9
ΔG^\ddagger_4	129.5 \pm 1.3	131.3 \pm 0.9	130.8 \pm 2.0
ΔG^\ddagger_5	129.7 \pm 0.9	133.2 \pm 0.7	131.5 \pm 0.8
ΔG^\ddagger_6	130.5 \pm 1.1	135.0 \pm 0.8	133.7 \pm 0.8
ΔG^\ddagger_7	130.3 \pm 2.4 ^a	133.7 \pm 2.7 ^a	132.0 \pm 3.3 ^a
(iv) <i>meso</i> -Tetrakis(2-iodo-5-methoxyphenyl)porphyrin (5)			
ΔG^\ddagger , kJ·mol $^{-1}$	temperature		
	423 K ^e	428 K ^e	435 K ^e
ΔG^\ddagger_1	143.5 \pm 1.3	145.8 \pm 0.8	145.0 \pm 0.9
ΔG^\ddagger_2	143.2 \pm 1.7	145.7 \pm 0.8	145.1 \pm 1.0
ΔG^\ddagger_3	146.2 \pm 5.5 ^f	153.9 \pm 1.4	142.8 \pm 0.8
ΔG^\ddagger_4	141.0 \pm 7.0 ^f	145.9 \pm 2.0	136.1 \pm 1.1
ΔG^\ddagger_5	142.6 \pm 1.1	147.1 \pm 0.8	145.7 \pm 0.9
ΔG^\ddagger_6	145.2 \pm 0.8	151.9 \pm 1.2	147.4 \pm 1.0
ΔG^\ddagger_7	143.6 \pm 2.3 ^a	148.4 \pm 5.7 ^a	143.7 \pm 6.7 ^a

^a ΔG^\ddagger_7 = average of ΔG^\ddagger_1 to ΔG^\ddagger_6 ; error reflects the range between the maximum and minimum values. ^b CDCl₃. ^c Toluene. ^d Xylene. ^e Mesitylene. ^f Not included in the calculation of ΔG^\ddagger_7 .

to the six rate constants defined in Figure 1 were obtained for each porphyrin at a given temperature (Table I). A similar analysis has been reported for the case of 5,10,15,20-tetrakis(*o*-cyanophenyl)porphyrin.⁷

Intuitively the six rates were expected to be very similar since one would expect the orientation of one aryl group to have little influence on the rotation of another, and this was observed (Table I). A contributing factor to the relatively large range in the data obtained for $X = I$ (5) may be slow decomposition of the iodo compound associated with prolonged heating at high temperatures.

The small variation among the ΔG^\ddagger 's determined for a given compound reflects the relative stabilities of the atropisomers. Deviations from the statistical concentrations at equilibrium were observed in hydrocarbon solvents, and, in particular, the concentration of the most polar and most sterically crowded $\alpha\alpha\alpha\alpha$ atropisomer decreased and the concentration of the least polar and sterically least hindered $\alpha\beta\alpha\beta$ atropisomer increased, with only small changes in concentrations of the other two atropisomers. Comparative experiments on 3 in toluene, xylene, and mesitylene indicated that in these solvents the equilibrium concentrations were identical, within experimental error, and differed considerably from those in dimethyl sulfoxide. Similar deviations from statistical concentrations at equilibrium have been reported in other ortho-substituted tetraarylporphyrins.^{1,4,6,7} Since our observations

Table II. Values of Σr^* for Ortho-Substituted Tetraarylporphyrins (\AA Angströms)


X	Y	d_x^a	d_y^a	$r_w(x)^b$	$r_w(y)^b$	d_{HX}^c	d_{HY}^c	Σr^*
H	H	1.03	1.03	1.20	1.20	0.86	0.86	3.08
F	H	1.32	1.03	1.47	1.20	0.58	0.86	3.63
Cl	H	1.70	1.03	1.75	1.20	0.28	0.86	4.21
Br	H	1.85	1.03	1.85	1.20	0.24	0.86	4.35
I	H	2.05	1.03	1.98	1.20	0.31	0.86	4.41
OH	H	1.36	1.03	1.52	1.20	0.55	0.86	3.71
<u>OCH₃</u> ^d	H	1.36	1.03	1.53	1.20	0.55	0.86	3.72
<u>CN</u>	H	2.27	1.03	1.51	1.20	0.48	0.86	3.77
<u>NHCOMe</u> ^d	H	1.32	1.03	1.58	1.20	0.58	0.86	3.74

^a d_x (d_y) = carbon-X (Y) bond length. ^b Van der Waals radii of groups X and Y; values of Bondi¹⁵ used in all cases, except NHCOMe and CN where values were obtained from ref 5. ^c Internuclear distance between pyrrolic hydrogen and X (Y). ^d Assuming atom underlined to be to the interacting group.

establish that the effect is solvent dependent, it can most probably be attributed to intermolecular solute-solvent interactions rather than being solely due to steric and electronic factors as proposed previously.^{4,6,7} The data indicate that further investigation of solvent effects would be informative, but in the present study the deviations from the expected statistical distribution of atropisomers have an insignificant effect on the size of the rotational barrier.

The measured rotational barrier represents the energy difference between the ground state of the molecule and the transition state for the rotation of the aryl ring about the aryl-porphyrin bond. In this study, the ground-state energies of the tetraarylporphyrins 1-5 were assumed to be substituent independent⁵ and negligible to a first approximation compared to the steric interactions that arise from the rotation of one of the four aryl rings about the aryl-porphyrin bond in the transition state. The geometric parameter Σr^* is defined as the "apparent overlap" of groups in a crowded transition state and affords a measure of steric interactions in internal rotations. For any two interacting groups the apparent interpenetration of atoms is the difference between the sum of their van der Waals radii and their internuclear distance. The parameter Σr^* is the sum of all such apparent interpenetrations in the transition state for a particular conformational change. The rotational barriers in ortho-substituted biphenyls (at 340 K) show a linear correlation with Σr^* according to eq 5,

$$\Delta G_{340}^{\ddagger} = 30.7 \Sigma r^* - 8.2 \text{ kJ}\cdot\text{mol}^{-1} \quad (5)$$

where r^* is in \AA .¹³ Values of Σr^* for porphyrins 1-5 were calculated from projections in the hypothetical planar transition states using X-ray data of 5,10,15,20-tetraphenylporphyrin¹⁴ for the bond lengths and angles, and the effective van der Waals radii of Bondi¹⁵ for the halogens. An example is shown in Figure 5. Σr^* values were also calculated for the other ortho-substituted tetraarylporphyrins for which kinetic data have been reported (Table II). The values obtained extend significantly the upper limit of the parameter from those values accessible in a biphenyl framework.

In order to compare the rotational barriers of porphyrins 1-5 with those of the biphenyls and test the generality of eq 5, it was

(13) Equation 5 was derived from the data in Table VI of ref 5 by a weighted linear least-squares analysis. Equation 1 of ref 5 is incorrect.

(14) Silvers, S. J.; Tulinsky, A. *J. Am. Chem. Soc.* **1967**, *89*, 3331. Bond angles and lengths were taken as the average of the reported values.

(15) (a) Bondi, A. *J. Phys. Chem.* **1964**, *68*, 441. (b) Bondi, A. *Ibid.* **1966**, *70*, 3006.

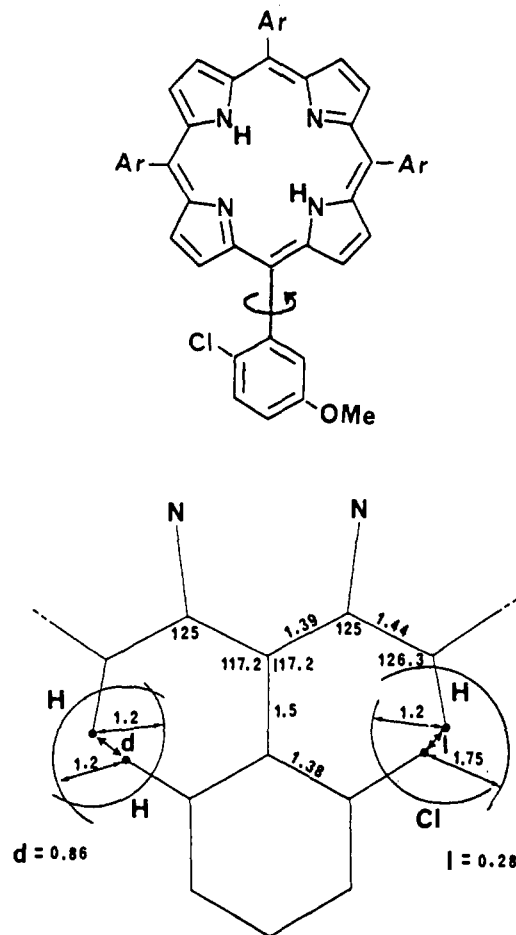


Figure 5. The contributions to Σr^* in 5,10,15,20-tetrakis(2-chloro-5-methoxyphenyl)porphyrin (3). All distances are in \AA , unspecified angles are 120° . $\Sigma r^* = [(1.2 + 1.2) - 0.86] + [(1.2 + 1.75) - 0.28]$.

necessary to extrapolate the porphyrin data to 340 K. Since data for the porphyrins were restricted to only three temperatures over a relatively narrow range, estimates of ΔS^\ddagger were not sufficiently reliable to permit accurate extrapolation of ΔG^\ddagger . For conformational changes which proceed via a hindered transition state, the magnitude of ΔS^\ddagger is typically small and negative. For example, in biphenyls, the average ΔS^\ddagger value⁵ was $-79 \pm 24 \text{ J}\cdot\text{K}^{-1}\cdot\text{mol}^{-1}$, while for atropisomerism in porphyrins, ΔS^\ddagger values of -40 and $-15 \text{ J}\cdot\text{K}^{-1}\cdot\text{mol}^{-1}$ have been reported.⁶ Using a value of $\Delta S^\ddagger = -60 \pm 50 \text{ J}\cdot\text{K}^{-1}\cdot\text{mol}^{-1}$, which encompasses most reported ΔS^\ddagger values for conformational changes such as those studied, an estimate of $\Delta G_{340}^{\ddagger}$ was obtained by extrapolation of ΔG^\ddagger from the middle of the temperature range where the experimental data were obtained. The experimental barriers and the values predicted at 340 K by use of eq 5 are given in Table III along with data available from other free-base ortho-substituted tetraarylporphyrins studies. Despite the assumptions necessary to provide $\Delta G_{340}^{\ddagger}$, there is good agreement between the estimated and the observed barriers, except in the case of the amido substituents. Effective sizes of these "large" amido groups have not been reported, and our calculations are based on data for the acetamido group, which probably underestimates the barrier.

The experimental values of $\Delta G_{340}^{\ddagger}$ (column 3, Table III excluding the amide entries), when plotted against Σr^* (column 9, Table II), also exhibit a linear relationship. The amide data were not included because of the uncertainty in the evaluation of Σr^* in these porphyrins. The weighted least-squares line of best fit (Figure 6, $r = 0.96$) to the data is given by:

$$\Delta G_{340}^{\ddagger} = 45.1 \Sigma r^* - 65.0 \text{ kJ}\cdot\text{mol}^{-1} \quad (6)$$

The results obtained (Table III) show that there is a similarity between steric stress (i.e., the energy penalty) and molecular deformation (Σr^*) in biphenyls and porphyrins. Thus, eq 5

Table III. Rotational Barriers in Ortho-Substituted Tetraarylporphyrins

substituent	ΔG^\ddagger_r kJ·mol ⁻¹ (see Table I) ^a	ΔG^\ddagger_{340} , kJ·mol ⁻¹ (exptl value)	ΔG^\ddagger_{340} , kJ·mol ⁻¹ (predicted from eq 5)	ref
F ^b	$\Delta G^\ddagger_{293} = 93.0 \pm 1.5$	95.8 ± 3.9^c	103	this work
Cl ^b	$\Delta G^\ddagger_{383} = 126.0 \pm 2.6$	123.4 ± 4.8^c	121	this work
Br ^b	$\Delta G^\ddagger_{403} = 132.0 \pm 2.8$	128.2 ± 5.9^c	125	this work
I ^b	$\Delta G^\ddagger_{428} = 145.2 \pm 4.9$	140 ± 9.3^c	127	this work
OH ^d	$\Delta G^\ddagger_{296} = 100.3 \pm 2.0$	103 ± 4.2^c	106	1
OCH ₃ ^d	$\Delta G^\ddagger_{433} = 108.3 \pm 0.8$	103 ± 5.5^c	106	8
OCH ₃ ^e	$\Delta G^\ddagger_{433} = 105.3 \pm 0.8$	100 ± 1.0^c	106	8
CN ^d	$\Delta G^\ddagger_{323} = 110 \pm 2.0^f$	111 ± 2.9^c	108	7
NHCOEt ^d		121 ± 2.0^f	107 ^g	6
NHCOEtMe ₃ ^d		126 ± 2.0^f	107 ^g	6
NHCO(CH ₂) ₁₅ Me ^d		121 ± 2.0^f	107 ^g	6

^a ΔG^\ddagger at middle of temperature range studied \pm average error of ΔG^\ddagger at three temperatures studied. ^b 5,10,15,20-Tetrakis(2-X-5-methoxyphenyl)porphyrin. ^c Calculated using $\Delta S^\ddagger = 60 \pm 50$ J·K⁻¹·mol⁻¹ (see text). ^d 5,10,15,20-Tetrakis(2-X-phenyl)porphyrin. ^e 5,10,15,20-Tetrakis(2,4-dimethoxyphenyl)porphyrin. ^f Errors estimated to account for nonstatistical concentrations of atropisomers reported. ^g Predicted value using Σr^* for NHCOME (see text).

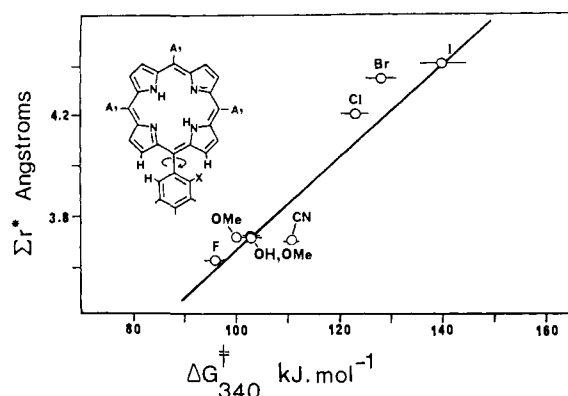


Figure 6. The correlation of ΔG^\ddagger_{340} with the sum of the apparent overlap (Σr^*) in ortho-substituted tetraarylporphyrins.

(derived for the biphenyls) can be used to predict rotational barriers in ortho-substituted tetraarylporphyrins for the range of porphyrins studied, but clearly eq 6 is more suitable for the prediction of rotational barriers in new porphyrins.

Conclusions

The kinetic stability of the atropisomers of tetraarylporphyrins can be correlated to the "steric size" of the ortho substituent. A semiquantitative measure of the barrier to rotation about the aryl-porphyrin bond can be made from the parameter Σr^* , the "apparent overlap" of the ortho substituents, which is determined by the van der Waals radii of the interacting substituents in a given framework. For a range of porphyrin derivatives, Σr^* is linearly related to the free energy of activation. The results of this work provide an effective method for the prediction of rotational barriers in tetraarylporphyrins and have potential application in the design of synthetically useful model porphyrins precursors for related chemical models for heme proteins.

Experimental Section

Melting points were determined on a Kofler micro melting point apparatus and are uncorrected. Proton NMR spectra were recorded on a Bruker WM 400-MHz spectrometer in deuteriochloroform (unless otherwise indicated), locked on solvent deuterium and referenced to the residual solvent protons. Routine ¹H NMR spectra were recorded on a Varian EM 390-MHz spectrometer. Fluorine spectra were recorded on a Varian XL 400-MHz spectrometer locked on solvent deuterium and referenced to trifluoromethyltoluene (δ -63 ppm) as the internal standard. Samples were ca. 0.02 M and were degassed. The spectrometer temperature was calibrated by the shift difference between the proton resonances in methanol.¹⁶ Ultraviolet spectra were recorded on a Hitachi 150-20 spectrometer in chloroform unless otherwise indicated. Infrared spectra were recorded on a Perkin-Elmer 710B spectrometer as liquid films. Mass spectra were recorded on an A.E.I. MS 902 spectrometer at 70 eV. Column chromatography was performed on Merck silica gel PF₂₅₄₊₃₆₆. Light petroleum refers to the fraction of bp 55-60 °C. Pyrrole

was freshly distilled before use. 5,10,15,20-Tetrakis(3-methoxyphenyl)porphyrin **17** was prepared by literature methods.

2-Iodo-5-methoxybenzaldehyde (6). A solution of iodine (8.9 g, 0.035 mol) in chloroform (400 mL) was added dropwise under nitrogen to a stirred suspension of *m*-methoxybenzaldehyde (5.0 g, 0.037 mol) and silver trifluoroacetate (7.8 g, 0.035 mol) over 2 h. The solution was stirred at room temperature for 18 h and the silver iodide removed by filtration. The filtrate was washed with aqueous sodium bisulfite and dried over magnesium sulfate; the solvent was removed to give a brown oily solid. Addition of ether precipitated a cream solid which was recrystallized from aqueous ethanol to give 2-iodo-5-methoxybenzaldehyde (**6**) as clear needles (1.9 g, 20%), mp 112-113 °C (lit.¹⁸ 114-115 °C). ¹H NMR (90 MHz): δ 3.82 (s, -OCH₃), 6.85 (dd, $J = 3.0$ and 8.7 Hz, H₄), 7.36 (d, $J = 3.0$ Hz, H₆), 7.74 (d, $J = 8.7$ Hz, H₃), 9.98 (s, -CHO).

2-Fluoro-5-methoxytoluene (8). 2-Amino-5-methoxytoluene (Aldrich, 15 g, 0.11 mol) in hydrochloric acid (3 M, 60 mL) was stirred and cooled to <5 °C. An ice-cold solution of sodium nitrite (8.3 g, 0.12 mol) in water (10 mL) was added at a rate such that the temperature remained between 0 and 5 °C. A cold solution of ammonium hexafluorophosphate (14 g, 0.11 mol) was added and the resultant diazonium salt collected and washed with cold water, ethanol, and ether. The pale pink solid (23 g) was finely ground with sand (50 g) and thoroughly dried before thermal decomposition. The mixture was heated intermittently with a Bunsen burner to maintain the evolution of white fumes and then cooled; the residue was extracted with chloroform. Removal of the solvent gave the crude product as a dark liquid which was purified by flash chromatography over silica (dichloromethane/light petroleum 1:5). The major nonpolar component was collected, the solvent removed, and the pale yellow residual liquid distilled to give 2-fluoro-5-methoxytoluene (**8**) as a clear liquid (7.6 g, 50%), bp 172-175 °C. Anal. Calcd for C₈H₉OF: C, 68.6; H, 6.5. Found: C, 68.9; H, 6.5. Visible spectrum (ethanol): λ_{\max} 279 (ϵ 2560) nm. Infrared: ν_{\max} 1050, 1120, 1160, 1220, 1272, 1318 (m), 1422 (m), 1463 (w), 1500 (s), 1600 (w), 1950 (b) cm⁻¹. ¹H NMR: δ 2.27 (d, $J = 1.8$ Hz, CH₃), 3.85 (s, -OCH₃), 6.66 (ddd, $J = 3.1$, 6.2, and 9.0 Hz, H₄), 6.71 (dd, $J = 3.1$ and 6.2 Hz, H₆), 6.92 (dd, $J = 9.0$ Hz, H₃). Mass spectrum: m/z 140 (M⁺, 100%), 125 (M - CH₃), 107 (19), 97 (29), 77(14).

2-Fluoro-5-methoxybenzyl Bromide (9). A solution of 2-fluoro-5-methoxytoluene (**8**) (8.0 g, 0.06 mol) in carbon tetrachloride (100 mL) was treated with *N*-bromosuccinimide (10.3 g, 0.06 mol) and benzoyl peroxide (0.3 g, 1.2 mmol) under nitrogen. The solution was stirred and heated to reflux for 4 h. The solvent was removed and the residue taken up in ether. The organic phase was washed with water, hydrochloric acid (3 M), and water and dried over sodium sulfate; the solvent was removed to give a yellow liquid, which was chromatographed over silica (dichloromethane/light petroleum 1:1). The major band was collected and distilled to give 2-fluoro-5-methoxybenzyl bromide (**9**) as a pale yellow liquid (8.8 g, 71%), bp 115 °C (0.6 mm) (Kugelrohr). Anal. Calcd for C₈H₈OFBr: C, 44.0; H, 3.7. Found: C, 44.2; H, 3.9. Visible spectrum (ethanol): λ_{\max} 292 (ϵ 3077) nm. Infrared: ν_{\max} 880 (m), 1020 (s), 1150 (m), 1200 (sh), 1220 (s), 1280 (m), 1320 (w), 1420 (m), 1450 (m), 1490 (s), 1590 (w), 2930 (bw) cm⁻¹. ¹H NMR: δ 3.78 (s, -OCH₃), 4.47 (d, $J = 1.22$ Hz, -CH₂-), 6.80 (ddd, $J = 3.1$, 6.0, and 9.2 Hz, H₄), 6.88 (dd, $J = 3.1$ and 9.2 Hz, H₆), 6.97 (dd, $J = 9.2$ Hz, H₃). Mass spectrum:

(17) Dalton, S.; Milgrom, L. R.; Pemberton, S. M. *J. Chem. Soc., Perkin Trans. 2* **1980**, 370.

(18) Akgün, E.; Gliński, M. B.; Dhawan, K. L.; Durst, T. *J. Org. Chem.* **1981**, *46*, 2730.

m/z 218 (M^+ , ^{79}Br , 10%), 139 ($M - \text{Br}$, 100), 109 (28), 96 (25).

2-Fluoro-5-methoxybenzaldehyde (7). 2-Fluoro-5-methoxybenzyl bromide (9) (6 g, 0.027 mol) and sodium carbonate (3.5 g, 0.033 mol) were stirred at 45–50 °C in dimethyl sulfoxide (35 mL) under nitrogen for 21 h. The solution was extracted with ether (3 × 50 mL). The combined ether extracts were washed with water (5 × 200 mL), dried over sodium sulfate, and evaporated to dryness. The crude product was purified by flash chromatography (chloroform/light petroleum 2:3). The major band was collected, the solvent removed, and the residue distilled to give 2-fluoro-5-methoxybenzaldehyde (7) as a pale yellow liquid (2.9 g, 68%), bp 80 °C (0.9 mm). Anal. Calcd for $\text{C}_8\text{H}_7\text{O}_2\text{F}$: C, 62.3; H, 4.6. Found: C, 62.7; H, 4.8. Visible spectrum (ethanol): λ_{max} 219 (ϵ 12906), 249 (7511), 326 (2814) nm. Infrared: ν_{max} 1020 (m), 1140 (m), 1200 (s), 1260 (s), 1320 (w), 1390 (m), 1415 (m), 1480 (s), 1600 (w), 1680 (s), 2850 (bw) cm^{-1} . $^1\text{H NMR}$ ($\text{Me}_2\text{SO}-d_6$) δ 3.83 (s, $-\text{OCH}_3$), 7.10 (dd, $J = 9.2$ Hz, H_3), 7.15 (m, H_4), 7.3 (dd, $J = 3.1$ and 5.1 Hz, H_6), 10.34 (s, CHO). Mass spectrum: m/z 154 (M^+ , 100%) 153 (85), 125 (16), 83 (34).

5,10,15,20-Tetrakis(2-fluoro-5-methoxyphenyl)porphyrin (2). Pyrrole (0.74 g, 0.011 mol) in propionic acid (3 mL) and 2-fluoro-5-methoxybenzaldehyde (7) (1.7 g, 0.011 mol) in propionic acid (5 mL) were added dropwise, simultaneously, to boiling propionic acid (45 mL). The solution was boiled for 70 min and allowed to stand overnight. Filtration afforded a purple solid which was washed with methanol until the filtrate was colorless (30 mg, 1%). The filtrate was evaporated to dryness and chromatographed on silica (dichloromethane/light petroleum 1:1) to remove black polymeric material. The crude porphyrin thus obtained was rechromatographed in the same solvent system to give additional pure porphyrin (275 mg, 12.4%). Recrystallization of the combined products from dichloromethane/pentane afforded 5,10,15,20-tetrakis(2-fluoro-5-methoxyphenyl)porphyrin (2) as purple crystals, mp >300 °C. Anal. Calcd for $\text{C}_{48}\text{H}_{34}\text{N}_4\text{O}_4\text{F}_8$: C, 71.4; H, 4.2; N, 7.0. Found: C, 71.1; H, 4.1; N, 7.4. Visible spectrum: λ_{max} 417 ($\log \epsilon$ 5.58), 511 (4.27), 545 (3.59), 586 (3.75), 650 (3.17) nm. $^1\text{H NMR}$ (CD_2Cl_2) δ -2.84 (bs, NH), 3.942, 3.940, 3.939, 3.934, 3.929, 3.926 (6 s, ratio 1:1:2:2:1:1, $-\text{OCH}_3$), 7.35–7.40 (m, H_3), 7.45–7.52 (m, H_4), 7.67–7.74 (m, H_6), 8.95 (H_2). $^{19}\text{F NMR}$: δ -123.7 ($\alpha\alpha\alpha$), -123.8, -124.0, -124.6 (intensity 1:2:1, $\alpha\alpha\alpha\beta$), -124.2 ($\alpha\alpha\beta\beta$), -124.4 ($\alpha\beta\alpha\beta$). Mass spectrum: m/z 806 (M^+ , 100%), 807 ($M + 1$, 50), 808 ($M + 2$, 20). Partial separation of the atropisomers was achieved by chromatography on silica (dichloromethane/light petroleum 1:1) at <5 °C. The solvent was removed from various fractions at 0 °C (0.2 mm). The resultant solids were stored in liquid nitrogen prior to NMR analysis which indicated enhancement of the samples in each atropisomer.

5,10,15,20-Tetrakis(2-chloro-5-methoxyphenyl)porphyrin (3). 2-Chloro-5-methoxybenzaldehyde¹⁹ (6.0 g, 0.035 mol) in boiling propionic acid (6 mL) and pyrrole (2.4 mL, 0.035 mol) were added dropwise simultaneously to refluxing propionic acid (140 mL). The mixture was refluxed for 1 h and allowed to stand for 2 days. The product was filtered off and washed with methanol to give the $\alpha\alpha\beta\beta$ atropisomer of the title porphyrin as glistening purple crystals (77 mg, 1%). The filtrate was concentrated to 150 mL, diluted with methanol (400 mL) and filtered. The black residue was washed with methanol, until the filtrate was colorless, and purified by chromatography on silica (dichloromethane/light petroleum 3:2). The major pink band was collected and the solvent removed to give a mixture of the four atropisomers of 5,10,15,20-tetrakis(2-chloro-5-methoxyphenyl)porphyrin (3) which crystallized from dichloromethane/pentane as shiny purple needles (450 mg, 6%), mp >300 °C. Anal. Calcd for $\text{C}_{48}\text{H}_{34}\text{N}_4\text{O}_4\text{Cl}_4$: C, 66.07; H, 3.93; N, 6.42. Found: C, 66.82; H, 4.26; N, 6.30. Visible spectrum: λ_{max} 418 ($\log \epsilon$ 5.61), 512 (4.29), 542 (3.54), 587 (3.78), 643 (2.99) nm. $^1\text{H NMR}$ ($\text{Me}_2\text{SO}-d_6$): δ -2.89 (bs, $-\text{NH}$), 3.883, 3.888, 3.896, 3.898, 3.912 (5 s, $-\text{OCH}_3$), 7.46 (m, H_4), 7.806, 7.811, 7.83, 7.834, 7.856, 7.868 (6 d, $J = 8.8$ Hz, H_3), 7.740, 7.783, 7.836, 7.868, 7.922, 7.955 (6 d, $J = 3.1$ Hz, H_6), 8.76 (s, H_2). Mass spectrum: m/z 870 (M^+ , 73%), 872 ($M + 2$, 100), 874 ($M + 4$, 66), 876 ($M + 6$, 24), 878 ($M + 8$, 6), 835 (9), 837 (11), 839 (6). The four atropisomers were separated by chromatography over silica (dichloromethane/light petroleum 3:5). The fractions purest in each atropisomer were rechromatographed in the same solvent system. In this way, each of the atropisomers was obtained in >95% purity. In order of elution these were the following. $\alpha\beta\alpha\beta$: $^1\text{H NMR}$ ($\text{Me}_2\text{SO}-d_6$) δ -2.79 (bs, NH), 3.950 (s, $-\text{OCH}_3$), 7.34 (dd, $J = 3.1$ and 8.8 Hz, H_4), 7.72 (d, $J = 8.8$ Hz, H_3), 7.78 (d, $J = 3.1$ Hz, H_6), 8.79 (s, H_2). $\alpha\alpha\beta\beta$: $^1\text{H NMR}$ ($\text{Me}_2\text{SO}-d_6$) δ -2.78 (bs, $-\text{NH}$), 3.917 (s, $-\text{OCH}_3$), 7.34 (dd, $J = 3.1$ and 8.8 Hz, H_4), 7.74 (d, $J = 8.8$ Hz, H_3), 7.74 (d, $J = 3.1$ Hz, H_6), 8.79 (s, H_2). $\alpha\alpha\alpha\alpha$: $^1\text{H NMR}$ ($\text{Me}_2\text{SO}-d_6$) δ -2.78 (bs, $-\text{NH}$), 3.908, 3.917, 3.922 (3 s, intensity 1:2:1, $-\text{OCH}_3$), 7.42 (m, spacings 3.1 and 8.8 Hz, H_4), 7.68, 7.90, 7.93 (3 d, intensity 1:2:1, $J = 3.1$ Hz, H_6),

7.97, 7.99, 8.02 (3 d, intensity 1:2:1, $J = 8.8$ Hz, H_3), 8.75 (m, H_2). $\alpha\alpha\alpha\alpha$: $^1\text{H NMR}$ ($\text{Me}_2\text{SO}-d_6$) δ -2.78 (bs, $-\text{NH}$), 3.912 (s, $-\text{OCH}_3$), 7.33 (dd, $J = 3.1$ and 8.8 Hz, H_4), 7.68 (d, $J = 3.1$ Hz, H_6), 7.74 (d, $J = 8.8$ Hz, H_3), 8.79 (s, H_2). The four atropisomers had identical visible spectra: λ_{max} 418 ($\log \epsilon$ 5.61), 512 (4.29), 542 (3.54), 587 (3.78), 643 (2.99) nm.

5,10,15,20-Tetrakis(2-bromo-5-methoxyphenyl)porphyrin (4). The title porphyrin was prepared as for the chloro derivative 3 in 8% crude yield from 2-bromo-5-methoxybenzaldehyde²⁰ and pyrrole. Purification was effected by chromatography on silica (dichloromethane/light petroleum 1:1). The major pink bands were collected and evaporated to dryness. Recrystallization from dichloromethane/pentane gave 5,10,15,20-tetrakis(2-bromo-5-methoxyphenyl)porphyrin (4) as shiny purple crystals, mp >300 °C. Anal. Calcd for $\text{C}_{48}\text{H}_{34}\text{N}_4\text{O}_4\text{Br}_4$: C, 54.9; H, 3.2; N, 5.3. Found: C, 55.1; H, 3.5; N, 5.3. Visible spectrum: λ_{max} 420 ($\log \epsilon$ 5.64), 514 (4.33), 544 (3.53), 588 (3.82), 645 (3.01) nm. $^1\text{H NMR}$: δ -2.83 (bs, $-\text{NH}$), 3.88, 3.89, 3.895, 3.90, 3.92 (5s, $-\text{OMe}$), 7.40 (m, H_4), 7.71, 7.79, 7.82, 7.89, 7.92, 8.00 (6 d, $J = 3.1$ Hz, H_6), 7.95, 7.96, 7.97, 7.98, 8.00, 8.01 (6 d, $J = 8.8$ Hz, H_3), 7.77 (s, H_2). Mass spectrum: m/z 1046 (M^+ , 2%), 1048 ($M + 2$, 4.4), 1050 ($M + 4$, 8), 1052 ($M + 6$, 7), 1002 (2), 1004 (3), 1006 (3), 1008 (2), 968 (3), 970 (3), 69 (100). The atropisomers were separated by chromatography on silica (dichloromethane/light petroleum 1:1). Four bands were collected and rechromatographed in the same solvent system. Removal of the solvent afforded the individual atropisomers in >95% purity as purple solids. In order of elution these were the following. $\alpha\beta\alpha\beta$: $^1\text{H NMR}$ ($\text{Me}_2\text{SO}-d_6$) δ -2.83 (bs, $-\text{NH}$), 3.950 (s, $-\text{OCH}_3$), 7.41 (dd, $J = 3.1$ and 8.8 Hz, H_4), 7.96 (d, $J = 8.8$ Hz, H_3), 8.07 (d, $J = 3.1$ Hz, H_6), 8.75 (s, H_2). $\alpha\alpha\beta\beta$: $^1\text{H NMR}$ ($\text{Me}_2\text{SO}-d_6$) δ -2.83 (bs, $-\text{NH}$), 3.913 (s, $-\text{OCH}_3$), 7.42 (dd, $J = 3.1$ and 8.8 Hz, H_4), 7.84 (d, $J = 3.1$ Hz, H_6), 8.00 (d, $J = 8.8$ Hz, H_3), 8.74 (s, H_2). $\alpha\alpha\alpha\beta$: $^1\text{H NMR}$ ($\text{Me}_2\text{SO}-d_6$) δ -2.83 (bs, $-\text{NH}$), 3.888, 3.911, 3.935 (3 s, intensity 1:2:1, $-\text{OCH}_3$), 7.42 (m, spacings 3.1 and 8.8 Hz, H_4), 7.68, 7.90, 7.93 (3 d, intensity 1:2:1, $J = 3.1$ Hz, H_6), 7.97, 7.99, 8.02 (3 d, intensity 1:2:1, H_3), 8.75 (s, H_2). $\alpha\alpha\alpha\alpha$: $^1\text{H NMR}$ ($\text{Me}_2\text{SO}-d_6$) δ -2.88 (bs, $-\text{NH}$), 3.925 (s, $-\text{OCH}_3$), 7.43 (dd, $J = 3.1$ and 8.8 Hz, H_4), 7.80 (d, $J = 3.1$ Hz, H_6), 8.02 (d, $J = 8.8$ Hz, H_3), 8.75 (s, H_2). The four atropisomers had identical visible spectra: λ_{max} 420 ($\log \epsilon$ 5.64), 514 (4.33), 544 (3.53), 588 (3.82), 645 (3.01) nm.

5,10,15,20-Tetrakis(2-iodo-5-methoxyphenyl)porphyrin (5). Pyrrole (1.75 g, 0.026 mol) was added dropwise to a refluxing solution of 2-iodo-5-methoxybenzaldehyde (6) (6.6 g, 0.025 mol) in propionic acid (110 mL). The solution was boiled for 1 h and allowed to stand overnight. The solution was filtered and the residue washed with methanol until the filtrate was colorless. The crude porphyrin was chromatographed on silica (dichloromethane) to remove polar impurities; the major pink band was collected and evaporated to dryness (230 mg, 3%). Recrystallization from dichloromethane/pentane afforded a mixture of the four atropisomers of 5,10,15,20-tetrakis(2-iodo-5-methoxyphenyl)porphyrin (5) as fine purple crystals (200 mg, 2.6%), mp >300 °C. Anal. Calcd for $\text{C}_{48}\text{H}_{34}\text{N}_4\text{O}_4\text{I}_4$: C, 46.55; H, 2.77; N, 4.53. Found: C, 45.84; H, 3.24; N, 4.26. Visible spectrum: λ_{max} 424 ($\log \epsilon$ 5.74), 518 (4.44), 548 (3.66), 592 (3.93), 657 (3.18) nm. $^1\text{H NMR}$ ($\text{Me}_2\text{SO}-d_6$) δ -2.72 (bs, $-\text{NH}$), 3.87, 3.88, 3.89, 3.91, 3.93, 3.94 (6 s, $-\text{OCH}_3$), 7.70, 7.71, 7.82, 7.89, 7.94, 8.12 (6d, $J = 2.9$ Hz, H_6), 8.130, 8.166, 8.167, 8.172, 8.186, 8.204, 8.212 (6d, $J = 8.8$ Hz, H_3), 8.68, 8.69 (2s, H_2). The four atropisomers were separated by chromatography on silica (dichloromethane/light petroleum 1:1). Each atropisomer, on removal of the solvent, was washed with methanol to give in >95% purity the pure isomers as purple solids. In order of elution these were the following. $\alpha\beta\alpha\beta$: $^1\text{H NMR}$ ($\text{Me}_2\text{SO}-d_6$) δ -2.71 (bs, $-\text{NH}$), 3.95 (s, $-\text{OCH}_3$), 7.26 (dd, $J = 2.9$ and 8.8 Hz, H_4), 8.11 (d, $J = 2.9$ Hz, H_6), 8.15 (d, $J = 8.8$ Hz, H_3), 8.69 (s, H_2). $\alpha\alpha\beta\beta$: $^1\text{H NMR}$ ($\text{Me}_2\text{SO}-d_6$) δ -2.72 (bs, $-\text{NH}$), 3.90 (s, $-\text{OCH}_3$), 7.25 (dd, $J = 2.9$ and 8.8 Hz, H_4), 7.82 (d, $J = 2.9$ Hz, H_6), 8.19 (d, $J = 8.8$ Hz, H_3), 8.69 (s, H_2). $\alpha\alpha\alpha\beta$: $^1\text{H NMR}$ ($\text{Me}_2\text{SO}-d_6$) δ -2.72 (bs, $-\text{NH}$), 3.87, 3.91, 3.93 (3s, intensity 1:2:1, $-\text{OCH}_3$), 7.25 (m, spacings 2.9 and 8.8 Hz, H_4), 7.71, 7.89, 7.94 (3 d, intensity 1:1:2, $J = 2.9$ Hz, H_6), 8.17, 8.18, 8.22 (3d, intensity 1:2:1, $J = 8.8$ Hz, H_3), 8.67 (s, H_2). $\alpha\alpha\alpha\alpha$: $^1\text{H NMR}$ ($\text{Me}_2\text{SO}-d_6$) δ -2.74 (bs, $-\text{NH}$), 3.89 (s, $-\text{OCH}_3$), 7.69 (dd, $J = 2.9$ and 8.8 Hz, H_4), 8.11 (d, $J = 2.9$ Hz, H_6), 8.15 (d, $J = 8.8$ Hz, H_3), 8.69 (s, H_2). The four atropisomers had identical visible spectra λ_{max} 424 ($\log \epsilon$ 5.74), 518 (4.44), 548 (3.66), 592 (3.93), 657 (3.18) nm.

Kinetic Experiments. A typical experimental procedure was as follows: A disequibrated sample of porphyrin was dissolved in toluene, xylene, or mesitylene (ca. 5 mg/100 mL). The solution was stirred and heated at a regulated temperature ($\pm 2^\circ$). Aliquots (0.5 mL) were removed at time intervals and cooled to room temperature where no further isom-

erization occurred. Chromatography was performed on a Waters μ -Porasil column 7.8 mm i.d. \times 30 cm (dichloromethane/light petroleum 13:7). The amount of each atropisomer was determined using a Waters Model 450 UV detector (operating at λ 420 nm) and a Hewlett-Packard 3380A integrator recorder.

Acknowledgment. We thank the Australian Research Grants Committee for financial support (to M.J.C. and S.S.) and the Australian Government for a Commonwealth Postgraduate award (to M.M.H.).

Registry No. 1, 29114-93-0; 2, 105762-41-2; $\alpha\alpha\alpha\alpha$ -3, 105814-96-8; $\alpha\alpha\alpha\beta$ -3, 105728-93-6; $\alpha\alpha\beta\beta$ -3, 105814-99-1; $\alpha\beta\alpha\beta$ -3, 105816-42-0; $\alpha\alpha\alpha\alpha$ -4, 105816-41-9; $\alpha\alpha\alpha\beta$ -4, 105814-97-9; $\alpha\alpha\beta\beta$ -4, 105816-45-3; $\alpha\beta\alpha\beta$ -4, 105728-91-4; $\alpha\alpha\alpha\alpha$ -5, 105816-44-2; $\alpha\alpha\alpha\beta$ -5, 105814-98-0; $\alpha\alpha\beta\beta$ -5, 105816-43-1; $\alpha\beta\alpha\beta$ -5, 105728-92-5; 6, 77287-58-2; 7, 105728-90-3; 8, 2338-54-7; 9, 91319-42-5; *m*-methoxybenzaldehyde, 591-31-1; 2-amino-5-methoxytoluene, 102-50-1; 2-methyl-4-methoxybenzenediazonium, 105728-89-0; hexafluorophosphate pyrrole, 109-97-7; 2-chloro-5-methoxybenzaldehyde, 13719-61-4; 2-bromo-5-methoxybenzaldehyde, 7507-86-0.

One-Electron Reduction of Daunomycin, Daunomycinone, and 7-Deoxydaunomycinone by the Xanthine/Xanthine Oxidase System: Detection of Semiquinone Free Radicals by Electron Spin Resonance

Jörg Schreiber,[†] Carolyn Mottley,^{†,‡} Birandra K. Sinha,^{†,‡} B. Kalyanaraman,[§] and Ronald P. Mason*[†]

Contribution from the Laboratory of Molecular Biophysics, National Institute for Environmental Health Sciences, Research Triangle Park, North Carolina 27709, and National Biomedical ESR Center, Department of Radiology, Medical College of Wisconsin, Milwaukee, Wisconsin 53226. Received June 30, 1986

Abstract: High-resolution electron spin resonance spectra of semiquinones from daunomycin and its derivatives, daunomycinone and 7-deoxydaunomycinone, have been obtained during reduction by xanthine/xanthine oxidase or dithionite in partially nonaqueous media. Hyperfine coupling constants were assigned with the help of an experiment in deuterated solvent to observe the exchangeable protons and with the help of computer routines for the automatic assignment of hyperfine coupling constants. In contrast, in buffer the ESR spectrum of the daunomycin was a single broad line and that of the 7-deoxydaunomycinone exhibited axial symmetry showing strong *g*-factor anisotropy. The differences in the ESR spectra of the daunomycin semiquinone and its derivatives and the effects of the nonaqueous solvents ethanol and dimethyl sulfoxide are discussed.

Daunomycin belongs to the widespread family of anthracycline drugs used in anticancer treatment. Because of the widespread use of daunomycin, a large number of investigations have been reported in recent years, and clinical as well as molecular aspects have been recently reviewed.¹⁻⁵ Since daunomycin is a quinone compound, it is a redox active molecule, one of its reaction pathways is the one-electron reduction to a semiquinone free radical. These radicals have been proposed to attack DNA site-specifically and produce strand breaks by producing reactive oxygen radicals such as the superoxide or the hydroxyl radical.^{6,7} Additionally, oxygen-derived free radicals have been proposed to be responsible for the use-restricting cardiotoxicity of the drug, which has been attributed to low levels of defensive enzymes against oxygen damage in the heart.⁸ Previously, the ESR technique of spin-trapping has been employed to detect daunomycin-dependent superoxide and hydroxyl radical formation.⁹⁻¹¹

Since daunomycin is an anthraquinone derivative and, like most quinones, is easily reduced to its semiquinone free radical, direct ESR has been used to detect semiquinones of daunomycin and its derivatives.¹⁰⁻¹⁴ Whereas the ESR spectra of enzymatically generated anthracycline semiquinones consist of a single, unresolved line,¹⁰⁻¹² those obtained from chemical reduction of anthracyclines¹³⁻¹⁶ reveal hyperfine structure. Because of this distinct difference in ESR spectra, there exists a structural dilemma as

to the true identity of the semiquinones derived from daunomycin, especially in enzymatic systems. In an attempt to resolve this, we have now undertaken a study involving enzymatic reduction of anthracyclines in solutions of buffer and dimethyl sulfoxide or ethanol.

We have chosen the xanthine/xanthine oxidase reduction system for the following reasons: (i) xanthine oxidase has previously been shown to be involved during myocardial reduction of anthracyclines,¹⁷ and (ii) the xanthine oxidase was still active in the presence of up to 50% dimethyl sulfoxide. We now report, for the first time,

- (1) Abdella, B. R. J.; Fisher, J. *Environ. Health Perspect.* **1985**, *64*, 3-18.
- (2) Arcamone, F. *Med. Res. Rev.* **1984**, *4*, 153-188.
- (3) Aubeil-Sadron, G.; Londos-Gagliardi, D. *Biochimie* **1984**, *66*, 333-352.
- (4) Favaudon, V. *Biochimie* **1982**, *64*, 457-475.
- (5) Young, R. C.; Ozols, R. F.; Myers, C. E. *N. Engl. J. Med.* **1981**, *305*, 139-153.
- (6) Bates, D. A.; Winterbourn, C. C. *Biochem. J.* **1982**, *203*, 155-160.
- (7) Winterbourn, C. C. *FEBS Lett.* **1981**, *136*, 89-94.
- (8) Doroshov, J. H. *Cancer Res.* **1983**, *43*, 4543-4551.
- (9) Lown, J. W.; Chen, H.-H. *Can. J. Chem.* **1981**, *59*, 390-395.
- (10) Gutiérrez, P. L.; Gee, M. V.; Bachur, N. R. *Arch. Biochem. Biophys.* **1983**, *223*, 68-75.
- (11) Kalyanaraman, B.; Peres-Reyez, E.; Mason, R. P. *Biochim. Biophys. Acta* **1980**, *630*, 119-130.
- (12) Sinha, B. K.; Gregory, J. L. *Biochem. Pharmacol.* **1981**, *30*, 2626-2629.
- (13) Kleyer, D. L.; Koch, T. H. *J. Am. Chem. Soc.* **1984**, *106*, 2380-2387.
- (14) Lown, J. W.; Chen, H.-H. *Can. J. Chem.* **1981**, *59*, 3212-3217.
- (15) Sinha, B. K.; Chignell, C. F. *Chem.-Biol. Interact.* **1979**, *28*, 301-308.
- (16) Sinha, B. K. *Chem.-Biol. Interact.* **1980**, *30*, 67-77.
- (17) Doroshov, J. H. *Cancer Res.* **1983**, *43*, 460-472.

[†] National Institute for Environmental Health Sciences.

[‡] Present address: Department of Chemistry, Luther College, Decorah, IA 52101.

[§] Present address: Laboratory of Clinical Pharmacology, National Cancer Institute, National Institutes of Health, Bethesda, MD 20205.

[§] Medical College of Wisconsin.